

We are IntechOpen, the world's leading publisher of Open Access books Built by scientists, for scientists

6,900

Open access books available

185,000

International authors and editors

200M

Downloads

Our authors are among the

154

Countries delivered to

TOP 1%

most cited scientists

12.2%

Contributors from top 500 universities



WEB OF SCIENCE™

Selection of our books indexed in the Book Citation Index
in Web of Science™ Core Collection (BKCI)

Interested in publishing with us?
Contact book.department@intechopen.com

Numbers displayed above are based on latest data collected.
For more information visit www.intechopen.com



A Tribo-Electrochemical Investigation of Degradation Processes in Metallic Glasses

Abdenacer Berradja

Additional information is available at the end of the chapter

<http://dx.doi.org/10.5772/intechopen.79387>

Abstract

Metallic glasses are relatively new materials with a large potential for applications in various technical and biomedical fields. However, for efficient use of these novel materials with an interesting combination of properties, it is necessary to fully characterize them for their mechanical and electrochemical properties. Studies on the effects of chemical parameters (pH, temperature, concentration of reagent) and tribological parameters (load, sliding speed, counterbody, contact configuration) on the kinetics of the reaction (i.e., the material removal rate) supply information on the dominant mechanisms governing the tribo-electrochemical behavior of metallic glasses. Although considerable efforts have been made to characterize their mechanical, corrosion, and magnetic properties, the study of their tribocorrosion patterns is in a rather unsatisfactory state, and very limited information is available. It is the purpose of this chapter to provide an overview of basic information on the tribo-electrochemical properties of most metallic glasses. This becomes crucial when such materials are to be considered in systems where solid surfaces are prone to mechano-chemical transformation processes.

Keywords: bulk metallic glasses, friction, wear-corrosion, synergy, tribocorrosion, tribo-electrochemistry

1. Introduction

Since the first discovery of amorphous alloys in the twentieth century, by Kramer [1] in the 1930s through vapor deposition, succeeded by Brenner et al. [2] in the 1950s through electrodeposition, and then by Klement et al. [3] in the 1960s through rapidly quenching casting processes (related to Au₇₀Si₃₀ glassy alloy system), several bulk glass-forming systems have emerged. Further innovation in this novel area of materials science has accredited a potential

market for commercial applications of metallic glasses. As a result, increased research on various tribological and corrosion properties of BMGs has occurred. The first published information on the corrosion properties of metallic glasses appeared in 1974 (it concerned the Fe-Cr-P-C alloy system) [4]. Since then, the corrosion behavior of all classes of metallic glasses and/or amorphous nanocrystalline alloys has been of great concern.

2. Corrosion resistance of bulk metallic glasses

The corrosion resistance is a critical factor for considering bulk metallic glasses (BMGs) used in hostile or chemical environments. However, there has been a growing interest in the corrosion behavior of these amorphous alloys.

At first presumption, many metallic glasses exhibit extremely good corrosion resistance, but there is a controversy over the exact mechanism(s) responsible for such improvement with respect to their crystalline counterparts. There are several possibilities for explaining the difference in corrosion behavior between amorphous and crystalline metals. The good corrosion resistance of single-phase glasses is often attributed to structure, composition, as well as structural and compositional homogeneity. Both the chemical homogeneity and the absence of microstructure in these amorphous alloys are most likely source of their superiority over their crystalline candidates. It has commonly been assumed that the very short solid-state diffusion time caused by the rapid cooling rates (as high as 10^6 K s^{-1}) required to produce the amorphous alloys, prevents the chemical heterogeneity and crystallization (but not always) [5].

When diffusion in the solid-state is kept faster and faster enough, the yielded homogeneous amorphous alloys should lack grain boundaries, dislocations, second-phase particles, segregates and other structural defects. These structural impurities are often present and commonly the culprits behind the localized corrosion (e.g., pitting, galvanic corrosion, etc.) observed in their crystalline counterpart alloys exposed to an aggressive environment. Corrosion readily occurs preferentially at such defect sites; therefore, metallic glasses can be expected to exhibit better corrosion resistance than crystalline alloys. Nevertheless, it has been shown that this statement does not always apply to BMGs [6]. Indeed, second phases (crystalline inclusions) were observed in some BMGs even after treatment. This was attributed to heterogeneous nucleation reactions caused by impurities in the melt that remained on the metal surface of the finished good [7].

Under normal working conditions, cathodes and anodes, possibly small but sufficiently large to cause localized corrosion, can be formed on the same metal glassy surface. Corrosion at the origin of these local crystalline inclusions will be greatly amplified upon conditions and can cause corrosion pits. This is one of the reasons why the persistent quest for BMG systems with increased glass-forming ability (i.e., decreased crystalline inclusions, see previous chapter) has provided the field with an influx of new alloying BMGs and compositions.

The ability of metals for alloying has provided the key to achieve enhanced properties, but certain elements are more common than others are. It is mainly the combined effect of the alloying elements, the test environment and, to some extent, earlier specific treatment

conditions, which determines the electrochemical properties profile of a number of metallic glasses. The addition of simple metals (SM), transition metals (early and late TM), and rare earth metals (REM) to the base metal was, inter alia, the principal strategy used to produce a selection of different metallic material glasses with a broad range of alloy compositions. According to IUPAC definition, a transition metal (TM) is defined as “a chemical element whose atoms have an incomplete d electronic sub-shell, or which can form cations whose electronic sub-shell d is incomplete.”

The early *versus* late transition metals differ generally in their oxidation states (each metal has different possible oxidation states). Electrons have a stronger attraction to the protons in the late transition metals (LTM), so the (LTM) form bonds that are harder to break.

Metallic glass alloys can be grouped into two major distinctive categories with intrinsically different corrosion behaviors, namely:

- The first group includes the TM-metalloid alloy systems. These alloys are usually the early transition metals (ETM): iron-, copper-, nickel-, cobalt-, zinc-, etc., and late transition metals (LTM): chromium-, zirconium-, titanium-, manganese-, lanthanum-, niobium-, scandium-, yttrium-, etc., base systems, and may normally contain approximately 20 at.% P, B, Si, and/or C as the metalloid component.
- The second class consists of binary, ternary or quaternary alloy system such as TM-SM, SM-TM-RE, and assorted SM-TM-X alloys. These alloys can contain a RE and/or TM and SM elements (such as aluminum, magnesium, beryllium, etc.).

2.1. Corrosion and associated mechanisms in the case of the transition metal-metal binary alloys

2.1.1. Fe-based BMG materials

One of the earliest studied systems in metallic glasses (MG), ranging from alloy design to material properties, is that of Fe-base alloys. These alloys can be formed as binary systems, such as Fe-B, or they may be much more complex, such as Fe-Ni-P-B quaternary systems, and even more intricate multiple systems. It has been suggested that the excellent resistance of certain iron metallic glass alloys to both uniform and localized corrosion results from their enhanced chemical reactivity relative to conventional stainless alloys [8]. The resistance to corrosion may be a result of the formation of a kind of passive film consisting of metallic and metalloid elements capable to strengthen the metallic glass surface against any specific chemical attack and under aggressive conditions (*cfr.* previous chapter).

In addition to the base metal, metallic glass alloys often contain appreciable concentrations of oxide film builder alloying elements to promote passivity, such as Cr, Ni, P, B as in the case of Fe-Ni-Cr-P-B system. They derive their corrosion resistance from similar shielding process as that of crystalline alloys, namely the development of a passive protective film (oxide scales). The significant difference between the corrosion-resistant metallic glass alloys and their crystalline counterparts, such as stainless steels, lies in the fact that the level of chromium necessary to promote passivity can be substantially less in the metallic glass alloys.

2.1.1.1. Effect of Cr content

One of the pioneer corrosion resistance studies on Fe-based amorphous alloys with P and C contents in acid chloride-based solutions was performed by Naka et al. [9]. Both uniform and localized corrosion resistances of these glassy alloys were mainly attributed to the growth of protective oxide films when appropriate additions of C and P are used [10]. A comparison was made between the corrosion rates of crystalline Fe-Cr alloys and amorphous Fe-Cr-P-C alloys as a function of chromium concentration as shown in **Figure 1**. At low chromium atomic content levels (<4 at.%), the amorphous alloy corrodes at a higher rate than the crystalline material. However, at even higher chromium levels (4 at.%), there is a significant decrease in the corrosion rate of the MG alloy, whereas the crystalline material remains unchanged. At more elevated and intermediate content Cr level (8 at.%), no corrosion was detected on the MG alloy by weight loss experiments after immersion for 168 h. Surprisingly, it was found that the concentration of HCl electrolyte, which has a significant effect on the corrosion behavior of the crystalline alloys, had no effect on the corrosion of the Fe-Cr-P-C or Fe-Ni-Cr-P-C base MG alloy systems, and which exhibited no weight loss after exposure for a period of 168 h [11].

Chromium was shown to be very effective to confer pitting resistance, such as for the metallic glass alloys Fe-Cr_xB₁₃C₇ and Fe-Cr_xB₁₃Si₇ in 3% NaCl [8]. With chromium level contents of 2 and 5 at.%, both MG alloy types suffered pitting at potentials more anodic than the free corrosion potential of approximately 0.6 V/SCE. The addition of 8 at.% Cr extended the pitting resistance nearly to 1 V/SCE, which represents an extreme condition of competition for alloys containing such a low level of chromium. By contrast, type 304 stainless steel contains

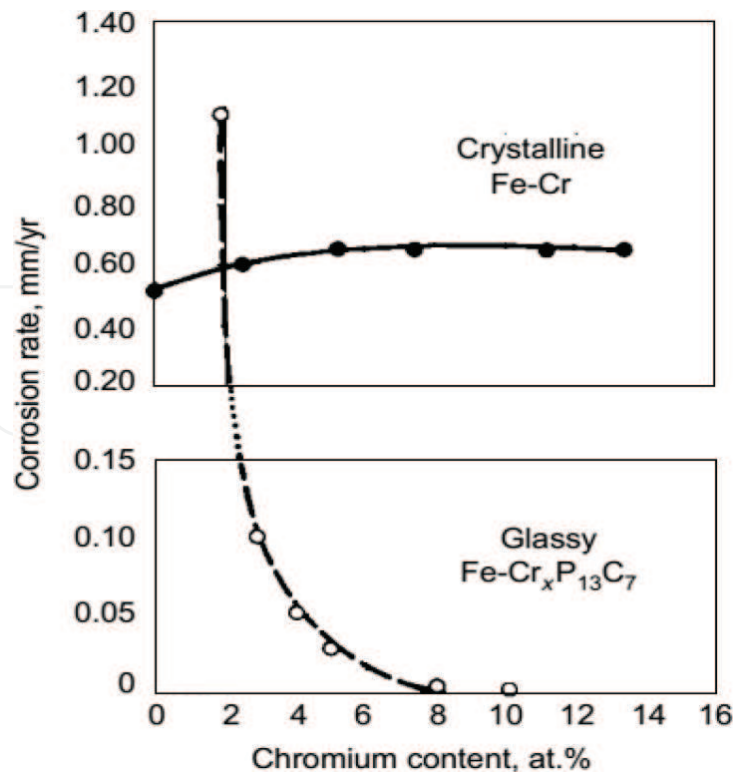


Figure 1. Comparison of the corrosion rates of glassy FeCrXP₁₃C₇ alloys and crystalline iron-chromium alloys in 1 N NaCl solution at 30°C. Reproduced from [11] with permission from Elsevier Science.

approximately 18 wt.% Cr, yet its pitting potential is several hundred millivolts less positive than that of the foregoing metallic glass alloys.

In another similar study, it has been shown that an increase of the Cr content from 0 up to 16 at.% in a series of Fe-Ni-Cr-P-B MG alloy filaments systems facilitated passivation in acidic electrolyte (1 N NaCl), and no pitting was observed on any of such alloy system polarized below the transpassive potential region [12]. However, polarization at transpassive potentials caused numerous pits to form that penetrated the MG alloy filament surface. Pits were found to be noncrystallographic in shape.

Pang et al. [13] investigated the corrosion behavior of bulk Fe₅₀-XCr₁₆Mo₁₆C₁₈BX alloys (X = 4, 6, and 8 at.%) in HCl solutions. The increase of B level content up to 8 at.% led to a decrease of the passive current density and to the reduction of the corrosion rate as well. Likewise, in other similar corrosion investigations reported elsewhere [13, 14], the Fe₄₃Cr₁₆Mo₁₆C₁₀B₅P₁₀ BMG exhibited a lower passive current density than that of Fe₄₃Cr₁₆Mo₁₆C₁₅B₁₀ BMG in a 1 M HCl electrolyte. However, in a 6 M HCl solution, and upon anodic polarization, the current density abruptly increases for the Fe₄₃Cr₁₆Mo₁₆C₁₅B₁₀ BMG, whereas the Fe₄₃Cr₁₆Mo₁₆C₁₀B₅P₁₀ BMG displayed a larger region of passive range with a passive current density of 100 mA m⁻², which makes it more effective in increasing the corrosion resistance compared to the former. A summary of these findings, which shows a decrease in the passive current density, and the expansion of the passive region as a function of B and P additions to Fe-based BMGs tested either in a 1 M HCl or in a 6 M HCl solution, is displayed in **Figure 2**.

2.1.1.2. Effect of Mo content

Molybdenum benefits the pitting resistance of metallic glass alloys and crystalline steels. The addition of Mo to glassy Fe-MoxP₁₃C₇ alloys suppressed pitting, decreased the critical current density for passivation and the passive current density [15]. As little as 4 at.% Mo prevented pitting corrosion in 1 N HCl; likewise, low additions of Mo were shown to be more effective in decreasing the corrosion rates than Cr. Molybdenum has been shown to facilitate the formation of a passive film of hydrated chromium or iron oxyhydroxide through its enrichment in the corrosion product layer during active dissolution [16]. The enrichment helps for the accumulation of passivating species in the film by lowering the dissolution rate of the species; the Mo-rich product subsequently dissolves, leaving little Mo behind in the film. However, in another case study [17], the increase of Mo content level up to 22.5 at.% was shown to be detrimental to the corrosion resistance of Fe-based BMG, more likely by increasing the risk of formation of secondary phases in the ferritic matrix zone.

2.1.1.3. Effect of other elements content (Ti, Zr, V, Nb, W, Mn, Co, Cu, Ru, Rh, Pd, Pt)

The effect of other alloying elements to Fe-based glass alloy on its corrosion resistance has been addressed in one study [18]. Hence, titanium, zirconium, vanadium, niobium, chromium, molybdenum, tungsten, manganese, cobalt, nickel, copper, ruthenium, rhodium, palladium, and platinum were all added to the Fe-X-P₁₃C₇ glassy alloy [18]. All elements, except manganese, decreased the corrosion rate of the iron glassy alloy in H₂SO₄, HCl, HNO₃, and

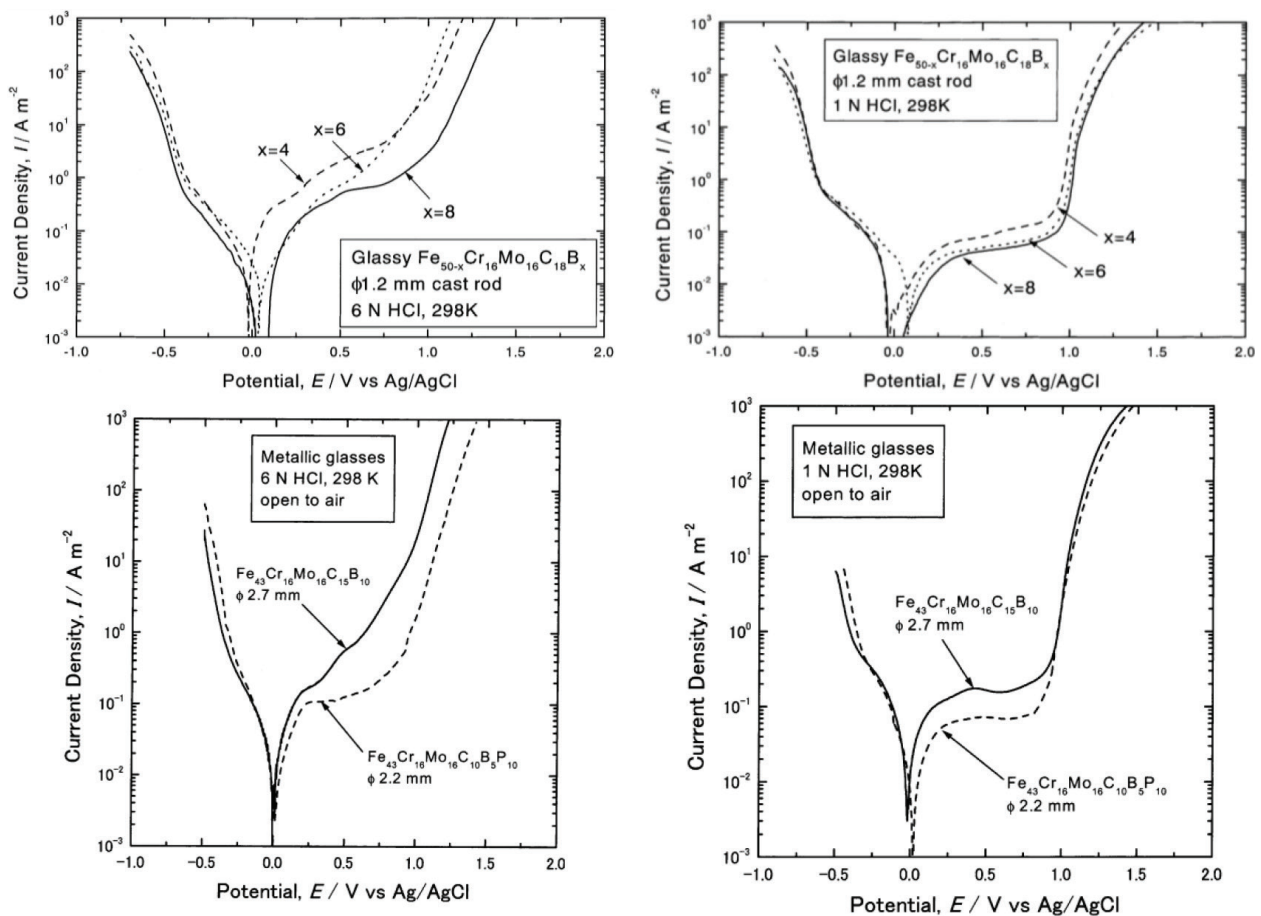


Figure 2. Potentiodynamic polarization curves of the cast glassy Fe-based BMGs (rods with a diameter of 1.2 mm) in 1 and 6 M HCl open to air at 298 K. Reproduced from [13, 29] with permission from Elsevier Science.

NaCl solutions. Although the base alloy, Fe-P13C7, did not passivate; additions of any of the foregoing elements at levels from 0.5 up to 40 at.% enabled passivation to occur during anodic polarization in 0.1 N H_2SO_4 . Chromium was the most efficient, still, molybdenum, and titanium were very beneficial. No pitting was observed in 3% NaCl for passivated alloys. The alloys that did not passivate, such as Fe-Co-P13C7, did not pit, but rather they dissolved uniformly.

Fe-W resisted to pitting corrosion up to 2.5 V/SCE in both acidic and neutral chloride solutions (pH 1 and 7, respectively) [19]. Addition of tungsten to Fe-WxP13C7 has the effect of increasing the critical pitting potential, E_{crit} to a level above 2 V/SCE for $x = 6$ at.%, but when $x = 10$ at.% of W was added it caused transpassive dissolution at 1 V/SCE of the MG alloy [19].

2.1.2. Ni-based BMG materials

Generally, Ni-based metallic glass systems exhibit a good resistance to uniform and localized corrosion. A number of investigations on the electrochemical characteristics of Ni-based amorphous alloys have been performed on ribbons [20–22] due to the struggle in producing amorphous bulk samples (i.e., having thickness > 1.5 mm). The elemental constituents that have typically been used to ensure a good corrosion resistance were either additions of metalloids such as P [20, 22] or additions of metals such as Ta [20, 21] and Nb [20].

Metallic glassy Ni-P has been recently investigated, which appeared to resist to chloride-induced corrosion [23]. In fact, its E -log (i) potentiodynamic behavior was basically identical whether in a chlorinated or chlorine-free environment. A form of chemical passivity has been proposed to explain its corrosion behavior. Passivation in the Ni-P system was mainly due to the formation of an ionic barrier layer rather than a classical passive oxide film. This barrier layer consists of hypophosphite ion adsorbed on the nickel phosphorous surface, with hydrogen/H₂O bonded outer layer. This barrier reaction layer inhibits the ion transport of water to the surface and thus prevents the hydration of nickel, which is the first step in the nickel dissolution process.

More recently, there have been growing efforts to decrease the additions of P due to its effective action on the loss of ductility of the Fe amorphous alloy [24]. Overall, the strategic approach that is found to be most effective in increasing the corrosion resistance depends on whether the solution is strongly oxidizing or not (e.g., 9 M HNO₃).

2.1.2.1. Effect of elements content (Ti, Zr, Ta, Nb, Cr, P)

There has been a consensus that additions of suitable metals to amorphous Ni-based alloys tend to increase their corrosion resistance. The electrochemical behavior of Ni-based amorphous alloys containing Ti, Ta, Zr, Nb, Cr, and/or P has been of a great concern for a number of investigators [20, 25–27]. One of the most significant studies was led by Shimamura et al. [20] who investigated the effect of P and other valve metals (e.g., Ta) on the corrosion properties of Ni-based amorphous ribbons immersed either in boiling 9 M HNO₃ solutions with and without any of Cr⁶⁺ ions content or in a boiling 6 M HCl electrolytes. Ta additions have been proven to be the most efficient in lowering the corrosion rates of Ni-based MG alloy. The addition of critical amounts of Ta resulted in undetectable corrosion rates (<10⁻³ mm year⁻¹). For example, after being immersed in a boiling 9 N HNO₃ solution for 168 h, the corrosion rate of Ni60Ti40 was estimated to be close to 1 mm year⁻¹. After adding of 30 at.% Ta, however, the Ni60Ti10Ta30 MG alloy exhibited an immune response to corrosion for the same period of exposure, i.e., 168 h. Immunity was attributed to the formation of a kind of a protective layer. Although, the authors Shimamura et al. [20] claimed that amorphous Ni-Ta alloys required more than 35 at.% Ta in a boiling 6 M HCl solution to form a tantalum oxyhydroxide (TaO₂[OH]) shielding passive film.

Alternatively, the addition of a small amount of P to Ni-Ta glassy alloys has been proven to be effective in significantly reducing their corrosion rates. The corrosion rate of Ni70Ta30 in a boiling 6 M HCl solution was more than 10⁴ times greater than that of Ni68Ta30P2 alloy when tested under similar conditions [20]. The authors believed that the addition of P promoted the growth of TaO₂(OH) passive film by accelerating selective dissolution of elements unnecessary for the passive film formation [20]. However, when experiments were performed in solutions with a high oxidizing power, the authors found that the addition of P to Ni-Ta alloys was not necessary to promote the growth of the passive film. Interestingly, many research works have suggested that a Ta-enriched passive film would probably be one of the reasons for the high corrosion resistance of Ni-based amorphous alloys in aggressive solutions [20, 21].

Moreover, it has been proven that the addition of approximately of 7 at.% Cr was sufficient to prevent pitting corrosion of Ni-Cr-P-B alloy systems immersed in 10% FeCl₃.H₂O at 30°C [27].

In another electrochemical study on the Ni-based MG alloy, Habazaki et al. [25] carried out potentiodynamic polarization tests on Ni₇₅-XCrXTa₅P₁₆B₄ BMGs (X = 5, 10, and 15 at.%) in a 6 M HCl solution in open air at 303 K. The passive current density was shown to decrease as the Cr (at.%) content increased in Ni₆₀Cr₁₅Ta₅P₁₆B₄.

Not all metal additions can improve the corrosion resistance of Ni-based alloys in aggressive solutions. This was the case for Cobalt. Pang et al. [26] studied the anodic polarization behavior of Ni₆₀-XCoXNb₂₀Ti₁₀Zr₁₀ (X = 0, 5, and 20 at.%) in a 6 M HCl solution. The Co additions did not significantly alter the polarization behavior; however, the three tested compositions exhibited spontaneous passivation in the 6 M HCl solution and no pitting was experienced during the anodic polarization. Passive current densities for the three tested alloys were almost identical, that is, about 10² mA m⁻². The beneficial effects behind the modification of Ni-based amorphous alloys are summarized in **Figure 3**.

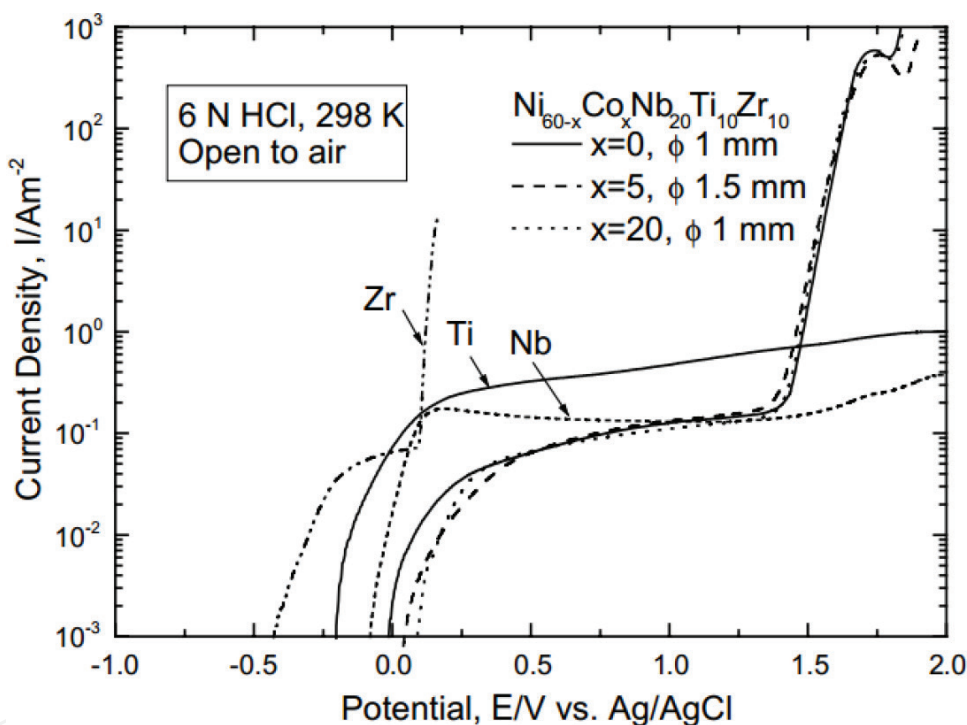


Figure 3. Anodic polarization curves of the bulk glassy Ni_{60-x}Co_xNb₂₀Ti₁₀Zr₁₀ alloys with their critical diameters for glass formation and pure niobium, titanium and zirconium in 6 N HCl solution open to air at 298 K. Reproduced from [26] with permission from Elsevier science.

2.1.3. Cu-based BMG materials

Recently, the corrosion behavior of either Cu, Zr, or Cu-Zr glassy alloy systems has been investigated [28]. The potentiodynamic anodic polarization behavior of the alloy system exhibited the characteristics of two components, namely Cu, and Zr, while the corrosion resistance of the alloy was not greater than that of the more passive (and noble) metal of the alloy, *viz.* zirconium [28]. Thus, it can be deduced that the corrosion resistance in some transition metal-metal alloy systems could seemingly be due to the presence of a key passivation element in the solid substitute solution, and not to the glassy structure.

In line with previous conclusions, and in order to better understand the origin of corrosion resistance in MT-MT systems, another supported corrosion study was carried out on alloys of Cu-Zr and Cu-Ti systems in H_2SO_4 , HCl, HNO_3 , and NaOH solutions [15]. In all solutions except the alkaline one, that is, NaOH, both crystalline and metallic glass Cu-Ti alloys exhibited corrosion rates lower than those of pure Cu, and in all cases, the corrosion resistance of the metallic glass alloy was better than that of the crystalline alloy. The metallic glass alloys in such compositional systems are not unusually corrosion-resistant; in fact, neither the crystalline nor the glassy forms of the alloys were more corrosion resistant than pure Ti or pure Zr. This may suggest that the presence of passivation elements, such as Ti, or Zr promotes the corrosion resistance of the metallic glass alloys, and therefore it cannot barely be the result of the presence of the glassy or vitreous state. These results are consistent with previous findings in that the corrosion resistance could be determined by the behavior of the most corrosion-resistant component of the glassy alloy in the transition metal-metal systems.

The synthesis of new bulk metallic glass alloys has subsequently extended the field of corrosion study of many alloy systems, including BMGs. Thus, the development of Cu-based BMGs has been a relatively new occurrence. Lin and Johnson [30] have successfully synthesized Cu-Zr-Ti-Ni glassy alloys with thicknesses of at least 4 mm. Afterward, Inoue et al. [31] developed Cu-Zr-Ti amorphous alloys containing at least 50 at.% Cu with critical diameters between 4 and 5 mm. Among the Cu-Ti glassy alloys, the Cu-Zr-Ti [32] and Cu-Hf-Ti [31] BMGs earned more attention because of their excellent mechanical properties (*viz.* compressive fracture strengths of 2.06–2.15 GPa), which put forward the concept of their possible usage as engineering materials.

The chemical resistance of Cu-BMG systems has become more and more interesting. Unfortunately, the corrosion resistance of most amorphous Cu-based bulk alloys has not been as impressive as their mechanical properties. Nevertheless, the influence of the content of the composition on the corrosion behavior of Cu-based BMGs with a variety of additions of elements is still in a continuous evaluation phase. Many of such additions have shown to improve the corrosion resistance of Cu-based BMGs [33–37, 39]. Additions of small amounts of Nb [33, 35, 36, 39] led to increase the corrosion resistance of Cu-based BMGs. The alloy with other elements such as Cr [34], Ta [33], or Mo [33, 34, 37] has also proved to be effective in improving the electrochemical properties of the Cu-base BMG systems (e.g., corrosion and pitting potentials, etc.). This was the case of one of the comparative studies conducted by Inoue, and Qin et al. [33, 35, 36], who evaluated the effect of low additions of Nb, Mo, and Ta (to a Cu-Zr-Ti-X (X = Nb, Mo, Ta)) on the corrosion behavior of the Cu₆₀Zr₃₀Ti₁₀ (at.%) BMGs exposed to solutions of 1 M HCl, 1 M HNO_3 , 1 M NaOH, or 0.5 M (3%) NaCl.

The typical potentiodynamic polarization curves of these Cu-based BMGs are shown in **Figure 4**. The electrochemical behavior of Cu_{59.4}Zr_{29.7}Ti_{9.9}Nb₁, Cu_{59.4}Zr_{29.7}Ti_{9.9}Mo₁, and Cu_{59.4}Zr_{29.7}Ti_{9.9}Ta₁ demonstrated that the addition of Nb was the most effective element in lowering the corrosion rate of Cu-based systems in all the test solutions considered. An increase in the Nb content (up to 5 at.%) led to a decrease in the rate of corrosion in all the solutions tested. As can be seen in **Figure 4**, the additions of Nb to Cu-base alloy resulted into more positive values of the E_{cor} , an indication of the improvement of its nobility, thereby suggesting a better behavior of corrosion resistance. This trend was supported by the lower

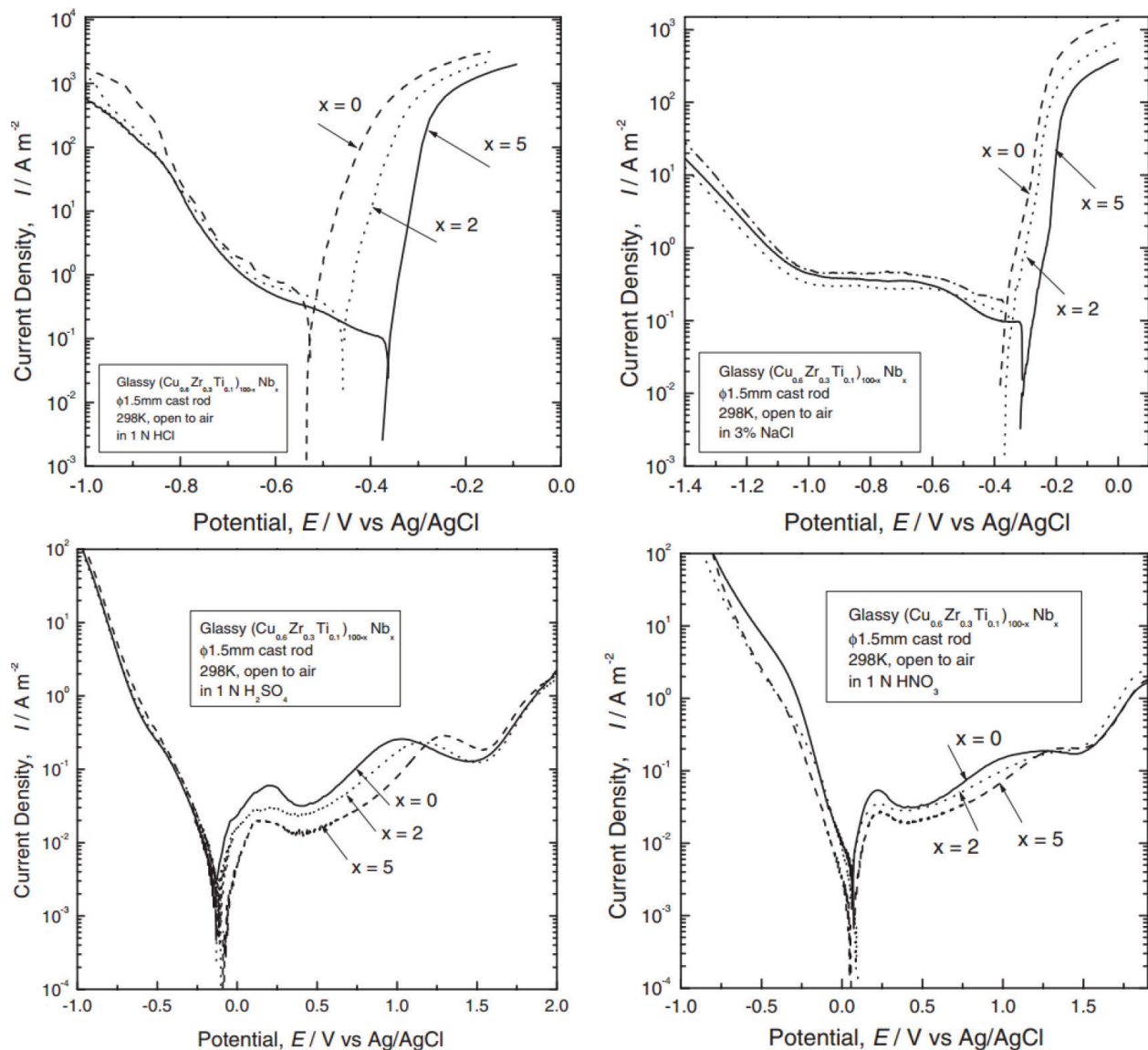


Figure 4. Potentiodynamic polarization curves of Cu-based BMGs ($\text{Cu}_{0.6}\text{Zr}_{0.3}\text{Ti}_{0.1}$) $_{100-x}\text{Nb}_x$ ($x = 0, 2$ and 6 at.%) alloys in either 1 N HCl , 0.5 M (3\% NaCl) , $1 \text{ N H}_2\text{SO}_4$ or 1 N HNO_3 open to air at 298 K . Reproduced from [35] with permission from Elsevier Science.

i_{cor} and the larger E_{pit} values. Ta was not to, as effective as Nb, more likely due to its lower concentration (only 0.2 at.% Ta was added).

Liu and Liu [34] investigated the electrochemical behavior of $\text{Cu}_{47}\text{Zr}_{11}\text{Ti}_{34}\text{Ni}_8$ and $(\text{Cu}_{47}\text{Zr}_{11}\text{Ti}_{34}\text{Ni}_8)_{99.5}\text{X}_{0.5}$ ($X = \text{Cr}, \text{Mo},$ and W) BMGs in aqueous solutions of $0.5 \text{ M H}_2\text{SO}_4$ and 1 M NaOH . Additions of Cr, Mo, and W have led to the extension of the passive region, the lowering of passive current densities, and lowered the corrosion rates. The alloy with Mo addition, however, showed the most improved corrosion resistance in the two tested solutions, namely H_2SO_4 and NaOH . All Cu-based BMGs with Mo additions had passive films enriched in ZrO_2 and TiO_2 but depleted in Cu-oxides, which are less chemically stable and denser than ZrO_2 and TiO_2 [37]. It was believed that the addition of Mo was most efficient in improving the corrosion resistance of the alloy because its lower ionization energy compared to that of Cr and W, and leading to faster film formation [34, 37].

Attention was paid to the dependence of the corrosion behavior of Cu-based BMGs on the test environment [33, 35, 36, 38, 39]. Different electrolytes have been selected to study this dependency. In their corrosion study of Cu-Zr-Al-Nb BMGs in 1 M HCl, 0.5 M NaCl, or 0.5 M H₂SO₄, and regardless of the composition, Tam et al. [38] showed that the corrosion rate of Cu-Zr-Al-Nb BMGs was higher in the case of more aggressive solutions (i.e., 1 M HCl and 0.5 M NaCl) and lower in the less aggressive solution (0.5 M H₂SO₄). In both solutions containing chloride ions, the Cu-BMGs exhibited active behavior, demonstrating the deleterious effects of chloride ions. However, an active-passive behavior was found in the case where Cu-BMGs were exposed to H₂SO₄. Similarly, Qin et al. [39] showed that either Cu-Zr-Al BMG or Cu-Zr-Al-Nb BMG exhibited an active behavior in a 0.5 M NaCl and escorted with high corrosion rates, and an active-passive response accompanied with low rates of corrosion in 0.5 M H₂SO₄ solution.

2.1.4. Zr-based BMG materials

So far, there have been only a few attempts to study the electrochemical properties of Zr-based BMGs in recent years. The majority of these studies have been devoted to systems such as Zr-Ni-Cu-Al [40], Zr-Ti-Ni-Cu-Be [41], and Zr-Ti-Ni-Cu [30] alloys. These Zr-based BMG families are attractive due to their good glass-forming ability and excellent mechanical properties.

Since then, the procedure of adding noble elements (e.g., Nb, Pd, Ti, Ta) has enabled it possible to develop new compositions of MG capable of improving both the capacity of glass-forming ability and the resistance to uniform and localized corrosion [42–45]. Raju et al. [45] investigated the corrosion behavior of Zr-Cu-Al-Ni-X (X = Nb or Ti up to 5 at.%) BMGs in low alkaline sulfate (0.1 M Na₂SO₄), and chloride electrolytes (0.01 M NaCl). Increasing the Nb or Ti content resulted in a slight decrease in E_{cor} and an increase in the passive current density in the sulfate solution. On the contrary, such an increase in the contents of Nb and Ti leads to an increase in the values of η_{pit} and η_p in the NaCl solution, thus revealing the improvement of the alloy *vis-a-vis* its corrosion resistance. A typical comparative graph of the anodic polarization curves of these related Zr-based BMGs in 0.1 M Na₂SO₄ electrolytes (pH 8) is shown in **Figure 5**.

In a similar study, Asami et al. [42] investigated the electrochemical behavior of Zr₆₀-XNbXAl₁₀Ni₁₀Cu₂₀ (X = 0, 5, 10, 15, and 20 at.%) BMGs in 0.5 M H₂SO₄ and 1 M HCl solutions. An increase in the concentration of Nb resulted in an increase in the E_{pit} . The η_{pit} however, did not always increase when the Nb content was increased. Substitution of 20 at.% of Nb for Zr resulted in a decrease in the rate of corrosion penetration (CPR) in the 1 M HCl solution from 100 down to 1 $\mu\text{m year}^{-1}$. The effectiveness of Hf addition (at.%) in improving the passivation ability of the Zr-Cu-Ni-Al BMG has been proven by Liu et al. [46]. Nevertheless, it was pointed out that the addition of noble metals does not always guarantee a better corrosion resistance of Zr-base BMGs.

Qin et al. [43] investigated the corrosion resistance of Zr-base bulk amorphous alloys with three different compositions, namely Zr₅₅Al₁₀Cu₃₀Ni₅-XPdX (with X = 0, 1, 3, and 5 at.%) in 0.6 M NaCl. Their findings have shown that the additions of Pd to the Zr-based MG lead to a decrease in the value of η_{pit} . Therefore, a change in the composition of Zr-based BMG does not always have a shielding effect for the MG alloy.

The effect of the environment is as challenging as that of alloying. It has been shown to play a significant role in the corrosion behavior of Zr-based bulk amorphous alloys. Gebert et al. [47]

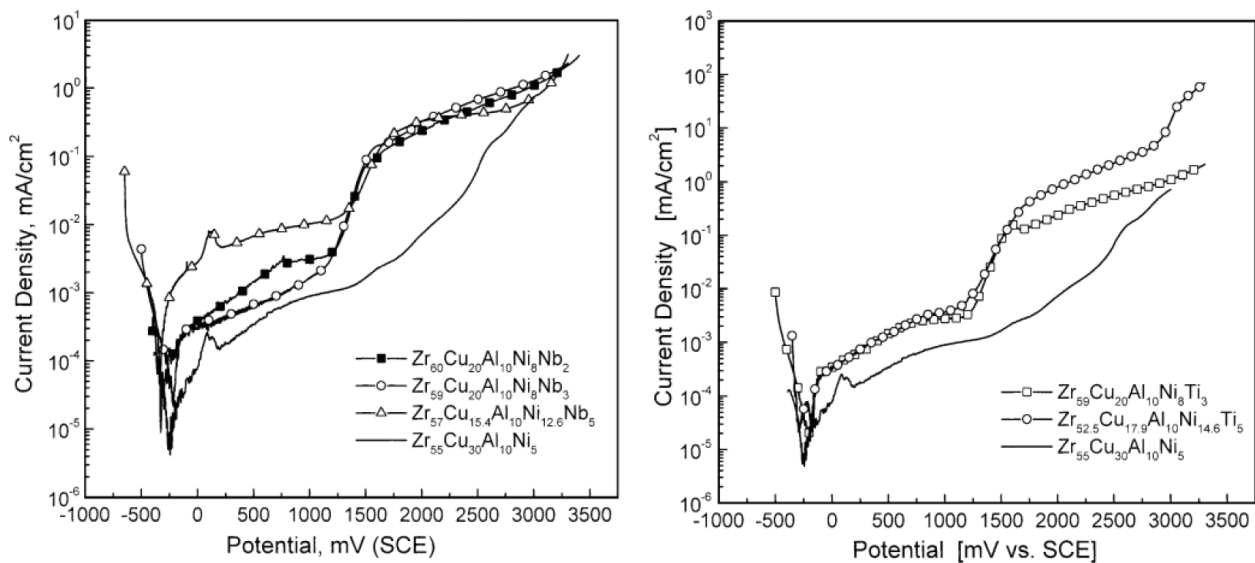


Figure 5. Anodic polarization curves of Zr-Cu-Al-Ni- x ($x = \text{Nb}$ or Ti) BMG alloys in 0.1 M Na_2SO_4 solution (pH 8). Reproduced from [45] with permission from Elsevier Science.

showed that the $\text{Zr}_{55}\text{Cu}_{30}\text{Al}_{10}\text{Ni}_5$ exhibited an immune response to localized corrosion either in a 0.1 M Na_2SO_4 or in a 0.1 M NaOH solution over the entire potential scanning range (-1000 up to 2000 mV/SCE). However, the susceptibility to pitting corrosion was observed on the BMG surface during anodic polarization experiments for chloride concentrations as low as 10^{-3} M. The E_{pit} was shown to decrease as the chloride concentrations increased. However, this trend has been tempered by the anodic pre-growth of a passive film. Similarly, Mudali et al. [48] have found that an increase in the concentration of NaCl of 0.01–0.2 M, added to a 0.5 M H_2SO_4 electrolyte, significantly decreased the E_{pit} of the Zr-base BMG. Other studies [47, 49] further support this outcome. It has been shown that a decrease in localized corrosion resistance is appropriately associated with the exposure of the Zr-base BMG surfaces to solutions with increasing concentrations of chloride ions [47, 49]. In agreement with the foregoing conclusions, many researchers [42, 44, 48, 50, 56] have concluded that the majority of the degradation of a number of Zr-based BMG systems due to localized corrosion involved exposure to solutions containing chloride ions while their best performance was satisfied in H_2SO_4 , Na_2SO_4 , and NaOH solutions.

The effect of other factors, despite what has been mentioned above, such as the test temperature and passivation level, was found to affect the electrochemical properties of Zr-based BMGs. Gebert et al. [50] studied this effect on the corrosion behavior of $\text{Zr}_{55}\text{Cu}_{30}\text{Al}_{10}\text{Ni}_5$ BMG. The anodic polarization was carried out at 298, 423 and 523 K in a 0.001 M NaCl electrolyte on the pre-passivated $\text{Zr}_{55}\text{Cu}_{30}\text{Al}_{10}\text{Ni}_5$ samples and those without any specific treatment. For untreated and pre-passivated BMG samples, the E_{pit} decreases with increasing temperature. It was concluded that a decrease in temperature and prior passivation treatment promoted the tendency of the $\text{Zr}_{55}\text{Cu}_{30}\text{Al}_{10}\text{Ni}_5$ BMG to resist pitting in the chloride solution, which was consistent with the observations of many crystalline and amorphous metal systems.

2.2. Corrosion and associated mechanisms in the case of the binary, ternary, or quaternary amorphous alloy systems

2.2.1. Other BMG-based system materials

The majority of previous corrosion studies involved BMG systems based on Cu, Fe, Ni, and Zr, but there are other BMG systems, such as Ca- [51] Mg- [52], and Ti-based MG [53] still under investigation.

The selection of materials and design alloys are, inter alia, the major factors driving the global BMGs market. More new BMG systems will emerge and become commercially available in mass production in the near future as these amorphous alloys have many attractive properties for everyday life such as biomaterials, electronic devices, structures, and so on. This is the case for Ca- and Ti-based BMGs, which have shown great interest because of their potential applications as biomaterials. The Mg-based system is interesting for applications requiring high strength with lightweight materials [54].

The electrochemical properties of Ca-based BMGs (Ca₆₅Mg₁₅Zn₂₀, Ca₅₅Mg₁₈Zn₁₁Cu₁₆, and Ca₅₀Mg₂₀Cu₃₀) were investigated in a 0.05 M Na₂SO₄ electrolyte [51]. The Ca₆₅Mg₁₅Zn₂₀ BMG experienced pitting at free corrosion conditions and had a CPR of 5691 μm year⁻¹. However, both Ca₅₀Mg₂₀Cu₃₀ and Ca₅₅Mg₁₈Zn₁₁Cu₁₆ were slightly passivated at E_{cor} conditions and exhibited CPR values in the order of 1503 and 311 μm year⁻¹ respectively.

The electrochemical behavior of the Ti_{43.3}Zr_{21.7}Ni_{7.5}Be_{27.5} BMG immersed in a phosphate buffered saline (PBS) solution at 310 K was examined by Morrison et al. [53]. The Ti-base BMG exhibited a passive behavior at E_{cor} conditions but it showed a localized corrosion susceptibility at more increasing potentials. The η_{pit} value was about 589 mV/SCE. The Ti-base BMG alloy had a CPR value of about 2.9 μm year⁻¹. The authors concluded that the alloy resistance to localized corrosion in the PBS solution was equivalent to or greater than that of the 316 L stainless steel when identical test conditions were prevailed.

Gebert et al. [52] has performed a comparative corrosion study of both Mg₆₅Y₁₀Cu₁₅Ag₁₀ and Mg₆₅Y₁₀Cu₂₅ BMGs in a borate buffer solution (pH 8.4) with pure Mg and Mg₆₅Y₁₀Cu₂₅ crystalline alloys. The electrochemical behavior of both amorphous and crystalline Mg₆₅Y₁₀Cu₂₅ alloys was similar, but superior to that of pure Mg. Although, the Mg₆₅Y₁₀Cu₁₅Ag₁₀ BMG exhibited superior corrosion resistance among the other three alloys.

2.2.2. Corrosion resistance of BMGs in comparison to crystalline alloys

There is still considerable interest in how the electrochemical properties of metallic glasses and BMGs compare to those of conventional crystalline alloys. Amorphous alloys are believed to exhibit corrosion resistance due to:

- their compositions, which are not constrained by the solubility limits, and they can be allied to elements promoting passivation [47],

- and their lack of microstructural characteristics, such as grain boundaries, dislocations, and precipitates, which commonly serve as sites for the local passive film breakdown entailing pitting.

Comparisons made on amorphous alloys and their crystalline counterparts allowed it possible to determine whether the structural disorder influences their corrosion behavior [55, 56]. Schroeder et al. [55] have shown that the resistance to pitting corrosion of the $Zr_{41.2}Ti_{13.8}Cu_{12.5}Ni_{10}Be_{22.5}$ BMG was nearly as equivalent as its crystalline counterpart when exposed to 0.5 M NaCl solution. However, the BMG was not more resistant to uniform corrosion in a 0.5 M $NaClO_4$ solution as its crystalline counterpart did. In accordance with this conclusion, Köster et al. [57] showed that there was no significant difference between the polarization behavior of the amorphous and nanocrystalline states of $Zr_{69.5}Cu_{12}Ni_{11}Al_{7.5}$ in a 0.1 N NaOH. However, Peter et al. [56] have found that the $Zr_{52.5}Cu_{17.9}Ni_{14.6}Al_{10}Ti_5$ BMG exhibited lower corrosion rates and greater resistance to pitting in a 0.6 M NaCl solution relative to their corresponding crystalline alloy of similar composition. Naka et al. [9] reported higher corrosion rates of amorphous Fe₇₀Cr₁₀B₂₀ (ribbon) in a 1 M HCl solution at 303 K relative to the crystalline Fe₉₀Cr₁₀ alloy. Nevertheless, the amorphous Fe₅₀Cr₃₀B₂₀ alloy experienced a lower corrosion rate in 1 M HCl than that of the Fe₇₀Cr₃₀ crystalline alloy. It has been cautioned that a convenient way to make an accurate assessment of the role of structural disorder on the corrosion behavior can only be achieved when the corrosion properties of the amorphous alloy have to be compared to those of a single-phased crystalline alloy of the same composition [58].

When considering the corrosion properties, the effect of the structure must also be addressed. However, the composition of the alloy is more likely to have a much greater influence on the electrochemical behavior of the alloy than if its structure is periodic or in a disordered state [58].

2.3. Tribological and tribocorrosion properties of BMGs

So far, limited literature information is available on the tribocorrosion properties of BMGs. Therefore, a brief overview is given below with respect to the recent major breakthrough in tribological and tribocorrosion performance of BMGs. The evaluation of metallic glasses as potentially applicable in situations where wear and corrosion act simultaneously is still premature.

Among the most important means of characterizing the performance of BMGs, materials scientists opt for the examination of the tribological and/or tribocorrosion resistance of a BMG material. The most studied material systems are zirconium-based bulk metallic glasses (Zr-BMGs) because of their wide use as mechanical components, their simple preparation process, and their excellent properties.

2.3.1. Zr-based BMGs

The tribocorrosion behavior of $Zr_{55}Cu_{30}Ni_5Al_{10}$ BMG sliding against AISI 52100 steel bearing in 3.5% NaCl solution in a pin-on-disk tribometer was evaluated by Ji et al. [59]. The wear volume loss of the $Zr_{55}Cu_{30}Ni_5Al_{10}$ BMG increased as the applied load (up to 20 N), the sliding distance and the sliding velocity (up to 1.5 m s^{-1}) increased. The BMG surface

structure was believed to evolve from an amorphous to a pseudo-crystalline nanostructure during sliding wear conditions. Due to the BMG surface crystallization, the wear resistance was improved and the friction coefficient (μ) of the Zr-based BMG-steel tribo-pair decreased from 0.5 to 0.08, but its free corrosion resistance has been lowered. It has also been shown that its degradation mechanisms evolve during sliding-corrosion tests as a function of normal load.

Abrasive wear was the dominant degradation mechanism at a load of 5 N, while adhesive and corrosive wear were predominant for an applied load of 20 N. Compared to AISI 304 stainless steel under similar test conditions, the Zr-based BMG has better tribocorrosion resistance in the NaCl solution but also beneficial in reducing the wear rate of the bearing steel disk. Therefore, the Zr-based BMG could be considered as a good candidate material for tribocorrosion in seawater applications.

2.3.1.1. Effect of the counter-body material

A recent study by Tian et al. [60] focused on the tribological properties of Zr-based BMG sliding against polymers, steels, and ceramics at various loads and speeds. Acoustic emission (AE) technology has been used to analyze the evolution of wear.

The coefficients of friction (μ) of the BMG sliding against either steel or ceramic balls were high (about 0.6–0.85) but decreased with increasing normal load and sliding velocity. As the steel balls were more ductile than the ceramic ones, the steel-BMG tribo-pairs generated weaker AE signals and exhibited larger wear rates. The main wear mechanism of the steel-BMG and ceramic-BMG pairs was dominated by a plastic flow of the BMG surface material caused by structural relaxation. The AE signals in a single frictional sequence decrease slightly with the increase of the sliding velocity due to the elastic energy consumed by the structural relaxation. The wear surfaces of Zr-based BMG samples were smoother, without crushing and peeling due to the super-plasticity of these BMGs over crystalline metallic materials.

Zr-based BMG sliding against polymer balls had much lower and more stable μ (0.5–0.65) than Zr-based BMG sliding against steel or ceramic balls. The low resistance to friction has been attributed to interfacial material transfer of polymer layers to the BMG surface during repeated sliding. The BMG sliding against polymer balls exhibited also the highest AE signals among the three types of counter-body materials considered, indicating that abrasive wear dominated the degradation mechanism in polymer-BMG tribo-pairs. Due to the low hardness and strength of the polymer counter-bodies, the BMG surfaces are not worn off. In addition to the abrasive wear mechanism in polymer-BMG tribo-pairs, a predominant process of adhesive wear was observed when the polymer wear debris (layers) were transferred to the BMG surfaces. Both the worn circular contact area and the wear volume loss of the polymer increased as the sliding distance increased. Similarly, plowing and fracture of the asperities increased after AE signals were found to increase in a single friction sequence. The authors call for the potential application of these types of BMGs in areas where tribology plays an important role. These Zr-based BMGs could act as new alternative candidates for tribo-materials (e.g., counter-body materials) over their traditional crystalline ones.

Zhong et al. [61] studied the tribological properties of Zr₄₁Ti₁₄Cu_{12.5}Ni₁₀Be_{22.5} pins sliding against different counter-body materials, namely AISI 5120 steel, AISI 52100 steel, and

Zr₄₁Ti₁₄Cu_{12.5}Ni₁₀Be_{22.5} amorphous alloys using a pin-on-disk tribometer at room temperature under relatively heavy loads. The μ depended on the counterbody material. The highest value of μ was measured for AISI 5120 steel (0.30) under a normal load of 150 N, whereas the lowest value (0.15) was recorded for the Zr-based BMG disk for a normal applied load of 100 N. The wear weight loss of the crystalline material disk was lower than that of the pins. The opposite result was obtained when the Zr-based BMG was used as the counterbody material. For the three different counterbody materials, the crystalline disks showed obvious piled-up material without severe peeling-off. In addition, microcracks were found on the AISI 5120 steel disk worn surface, whereas the plastic flow has become one of the dominant wear mechanisms on the AISI 52100 steel disk. However, rough detached surface damage and wave-like patterns accompanied by pronounced delamination have been found on the BMG pins when amorphous disks were used as counterpart. Differences in wear mechanisms have been observed between the crystalline materials and the amorphous disks. The wear mechanisms of Zr-based BMG pins included grooves, micro-cracks, peeling-off and vicious flow when they slid against crystalline materials.

2.3.1.2. Effect of the loading conditions

The tribological behavior of a Zr_{52.5}Cu_{17.9}Ni_{14.6}Al₁₀Ti₅ (at.%) BMG sliding against yttria-stabilized zirconia counterparts was investigated using pin-on-disk in two distinct environments, namely air and argon [62]. It was found that the wear of the Zr-based BMG was reduced by more than 45% due to the removal of oxygen from the test environment at two different loads, namely, 16 and 23 N. The surface wear pins were examined using X-ray diffractometry, differential scanning calorimetry, scanning electron microscopy and optical surface profilometry. A number of abrasive particles and grooves were observed on the worn surface of the pin tested in air, while a relatively smooth worn surface was found for specimens tested in argon. In ambient air, an abrasive wear mechanism dominates the degradation mechanism of the BMG pin, whereas, in argon, an adhesive wear controls the wear process.

The effect of the load on the wear behavior of Zr₅₅Cu₃₀Ni₅Al₁₀ BMG under linear reciprocating sliding conditions was investigated by Tao et al. [63]. An increase in the normal load results in a decrease of the μ of the Zr-based BMG (from 0.348 down to 0.226), and an increase of the wear volume loss. The wear mechanism evolves during friction, combining different processes such as welding, adhesive, and abrasive wear. At low loads, adhesive wear governs the degradation wear mechanism of the Zr-based BMG.

2.3.1.3. Effect of the test medium

The wear resistance of a Zr₆₁Ti₂Cu₂₅Al₁₂ (ZT1) BMG sliding against Si₃N₄ balls in dry (air), and lubricated states (deionized water, and simulated physiological media) in a ball-on-flat contact configuration was investigated by Wang et al. [64]. It has been shown that the wear resistance of ZT1 BMG in air and deionized water was superior to that of Ti6Al4V alloy but inferior to that of 316 L stainless steel and CoCrMo alloy when similar conditions were used. However, in simulated physiological media, such as phosphate buffered solution (PBS), and DMEM + FBS (Dulbecco's modified Eagle medium with 10 vol.% fetal bovine serum), the Zr-based BMG exhibited lower wear resistance than that of Ti6Al4V, 316 L stainless steel, and

CoCrMo. This was likely attributed to its moderate pitting corrosion resistance, and its poor depassivation-repassivation kinetics, as induced by passive film breakdown in the solution containing chloride ions during the tribo-corrosion conditions. The presence of proteins in the test solution had a significant effect on the rapid decrease in the pitting resistance of the Zr-based BMG, which caused greater and severe wear damage. Therefore, improvement in the pitting resistance of the Zr-based BMG in physiological media is necessary if it concerns its possible use as a biomedical implant. In addition, screening of a good material as a counterpart to coupling with Zr-based BMG is an additional key factor in ensuring better wear resistance (e.g., by lowering its wear rate). In dry conditions, abrasive wear was predominant mechanism in the case of ZT1 BMG. Under lubricated sliding conditions with the presence of deionized water, the wear damage caused by abrasion can be mitigated. In a simulated physiological environment with the presence of chloride ions, synergistic effects of abrasive and corrosive wear more likely control the wear process. For the four metals studied, the wear resistance had no distinct correlation with the hardness, while the material with high Young's modulus had better wear resistance.

In another investigation conducted by Hua et al. [65], the tribological behavior of a Zr₅₃Al₁₆Co_{23.25}Ag_{7.75} BMG in air and phosphate buffer saline (PBS) solution was evaluated using ball-on-disk reciprocating sliding contacts. A biomedical alloy Ti-6Al-4V was used for comparison purposes. The wear resistance of the Zr-Al-Co-Ag BMG sliding in air has been shown to be superior to that of Ti-6Al-4V alloy. Under such dry friction conditions, the wear damage on Zr-based BMG was governed by combined oxidational and adhesive wear processes, whereas the wear mechanisms on the Ti-6Al-4V alloy was mainly driven by conjoint processes of abrasion and adhesion damage. Similarly, under lubricated contact conditions, both oxidational and abrasive wear were the main wear mechanisms of the Ti-6Al-4V alloy in PBS. The Zr-based BMG exhibited lower wear resistance under lubricated sliding conditions (i.e., PBS) over dry friction, but higher than that of Ti-6Al-4V alloy. That low wear resistance was likely attributed to the low pitting corrosion resistance of Zr-Al-Co-Ag BMG in the medium containing chloride ions, and to the synergistic effects of abrasive and corrosive wear during the tribocorrosion tests. The pitting resistance in PBS solution of Zr-Al-Co-Ag BMG was lower than that of Ti-6Al-4V alloy, and was considered a key factor in the tribocorrosion behavior of the Zr-based BMG under the conditions considered.

2.3.2. Fe-based BMGs

The sliding wear behavior of a range of rapidly solidified alloy samples based on the composition of Fe₆₈Cr₁₈Mo₂B₁₂ (prepared by planar-flow casting) against a cobalt-bonded tungsten carbide counterface was evaluated using a modified crossed-cylinder wear testing rig [66]. A range of microstructures was examined, and the effect on the wear performance was evaluated. Alloys in ribbon forms were investigated in the as-cast amorphous state and after devitrification at various temperatures, and with the bulk-devitrified sample prepared by hot extrusion of the crushed ribbon. Low-temperature crystallization of the ribbon produced a high volume fraction of metastable Fe₃B in a ferritic matrix, whereas high-temperature crystallization produced M₂B and Mo-rich borides, still in a ferrite matrix. The wear results showed that the alloy having the stable M₂B and Mo-rich borides had the best wear performance, whereas that of the amorphous material had the highest wear rate, and the alloy with

Fe_3B precipitates exhibited an intermediate wear behavior. The wear volume was systematically higher for the amorphous alloy than for the corresponding devitrified material. This was believed to be the result of the continuous crystallization of the glassy ribbon on the worn surface. Crystallization produced a microstructure of deformed ferrite containing a uniform dispersion of very fine boride precipitates. The combination of extensive microcracks and the inability of the precipitates to support the load led to an increase in the wear rate.

3. Toward the use of BMGs for tribo-electrochemistry systems in biomedical applications

The unique properties of BMGs make these materials attractive alternatives in biomedical applications. However, the most promising strategies for biomedical applications are quite limited. BMGs have potential biomedical applications as screws due to their toughness and high strength. Moreover, it has been reported that certain BMG compositions have low magnetic susceptibility, which could be advantageous in surgical instrument applications for interventional magnetic resonance imaging (MRI) [67, 68]. The ease of micro-forming and manufacturing of BMGs [69] also lends itself to the production of gears for small, high-powered micromotors that could be of use in arthroscopic tools. Another promising application is the biofunctionalization technology. Biofunctionalization consists of adapting compounds, for example metals, to make them compatible with a biomedical application. Finally, one of the most promising biomedical applications of BMGs is the use in bone fracture fixation and hip arthroplasty. BMGs have a low modulus that is comparable to the modulus of the bone as well as a high strength to withstand the significant forces generated in the skeletal system of the human body.

In particular, the acceptability of BMGs as potential candidates for implants (e.g., load-bearing materials) in the human body is a very interesting and novel topic for a recent field of applications. To be effective, the BMGs should behave like biomaterials for the duration of their use. Above all, they should have sufficient mechanical strength, corrosion and wear resistance to withstand the harsh conditions of the body environment. If this is not achieved, degradation of the implant occurs and secondary effects take place leading to carcinogenicity, hypersensitivity, inflammation, and other complications. Recent investigations have claimed potential tribocorrosion performance of BMGs in simulated body fluids; however, improvements are needed to achieve full functioning.

The tribocorrosion performance of a Zr-based BMG, namely ZrCuAlNi, has recently been evaluated in different media simulating body fluids with and without the presence of proteins [70]. For comparison, a low-alloyed Zr material and a crystalline structure of the same alloy were also studied. It has been shown that the adsorption of the protein on the metal surface modifies both the cathodic and anodic electrochemical patterns and thus changes the prevailing reactions. The ZrCuAlNi BMG alloy in both structures, that is, amorphous and crystalline, did not form any stable passive film and an active dissolution in the anodic region was observed; only the presence of phosphates has generated a small passive plateau. The results also showed that the BMG material with amorphous structure had the largest wear rates in all electrolytes tested (i.e., NaCl, phosphate buffer solution, and phosphate buffer solution with protein), whereas the crystalline structure of the BMG showed negligible

wear rates. Two different tribocorrosion mechanisms were observed in the ZrCuAlNi BMG alloy. The amorphous structure suffered from wear-accelerated corrosion generating larger wear rates due to galvanic coupling effects. The crystalline structure did not suffer from wear accelerated corrosion (no galvanic coupling effects due to lack of passivity) and thus lower wear rates were measured. The amorphous BMG material generated a large amount of wear debris during tribocorrosion tests, which act as very abrasive particles, thereby entailing the wear of the counterpart material (alumina). This was due to the formation of grooves and the growth/breakdown sequences of an amorphous oxide film and the high availability of Zr in the material. Crystalline BMG material generated low amount of wear debris, which could be attributed to recrystallization (nano-crystallization), and the presence of a new intermetallic phase (Zr_2Cu), promoting an improvement of its mechanical properties under tribocorrosion conditions.

In another comparable study [71], using a reciprocating ball-on-disk tribometer equipped with an electrochemical cell, the degradation mechanisms due to mechanical wear and tribocorrosion of Zr-based BMGs, with nominal compositions of Zr55Cu30Ni5Al10 and Zr65Cu18Ni7Al10 used as potential load-bearing implant materials, were examined. The Zr65-BMG with a higher Zr content showed an increase in plasticity but a reduction in its wear resistance during sliding was noticed. Both BMGs experienced abrasive wear mechanisms after dry sliding wear test conditions (under applied load of 2 N). The worn surface had a higher hardness and no wear-induced recrystallization was confirmed *via* FIB cross-section analysis. Therefore, the hardening mechanism was due to the free-volume annihilation under suppressed shear deformation. The more passive nature of the Zr65-BMG had consequently a negative influence on its tribocorrosion resistance since wear-accelerated corrosion speeded-up its governing degradation mechanism. It has been shown that a galvanic coupling established between the depassivated wear track and the surrounding passive area was behind the main degradation mechanism of passive Zr65-BMG subjected to the tribocorrosion environment. In order to apply the BMGs for load-bearing biomedical devices, it is required to find out a balance between their wear-controlled mechanisms, namely wear-accelerated corrosion and static corrosion resistance.

Author details

Abdenacer Berradja

Address all correspondence to: a.berradja@gmail.com

MTM Department, K.U. Leuven, Leuven, Belgium

References

- [1] Kramer J. The amorphous state of metals. *Zeitschrift für Physik*. 1937;**106**:675-691
- [2] Brenner A, Couch DE, Williams EK. Electrodeposition of alloys of phosphorus with nickel or cobalt. *J. Research of the National Bureau of Standards*. 1950;**44**:109

- [3] Klement W, Willens RH, Duwez P. Non-crystalline structure in solidified gold-silicon alloys. *Nature*. 1960;**187**:869-870
- [4] Naka M, Hashimoto K, Masumoto T. Corrosion resistance of amorphous iron alloys with chromium. *J. Japan Institute of Metals*. 1974;**38**(9):835-841
- [5] Hays CC, Kim CP, Johnson WL. Microstructure controlled shear band pattern formation and enhanced plasticity of bulk metallic glasses containing in situ formed ductile phase dendrite dispersions. *Physical Review Letters*. 2000;**84**:2901-2904
- [6] Inoue A, Kimura HM, Sasamori K, Masumoto T. Ultrahigh strength of rapidly solidified Al-(96-x), Cr-3, Ce-1, Co-x (x = 1, 1.5 and 2%) alloys containing an icosahedral phase as a main component. *Materials Transactions*. 1994;**35**:85
- [7] Flores KM, Dauskardt RH. Enhanced toughness due to stable crack tip damage zones in bulk metallic glass. *Scripta Materialia*. 1999;**41**:937-943
- [8] Hashimoto K, Naka M, Masumoto T. Scientific Report of the Research Institutes of Tohoku University, A-26. Tohoku University; 1976. p. 48
- [9] Naka M, Hashimoto K, Masumoto T. Corrosion resistivity of amorphous Fe alloys containing Cr. *Journal of the Japan Institute of Metals*. 1974;**38**(9):835-841
- [10] Masumoto T, Hashimoto K. Chemical properties of amorphous metals. *Annual Review of Materials Science*. 1978;**8**:215-233
- [11] Naka M, Hashimoto K, Masumoto T. High Corrosion Resistance of Chromium-Bearing Amorphous Iron Alloys in Neutral and Acidic Solutions Containing Chloride. *Corrosion*. 1976;**32**(4):146-152
- [12] Diegle RB. Localized Corrosion of Amorphous Fe-Ni-Cr-P-B Alloys. *Corrosion*. 1979; **35**(6):250-258
- [13] Pang SJ, Zhang T, Asami K, Inoue A. Bulk glassy Fe-Cr-Mo-C-B alloys with high corrosion resistance. *Corrosion Science*. 2002;**44**(8):1847-1856
- [14] Asami K, Pang SJ, Zhang T, Inoue A. Preparation and corrosion resistance of Fe-Cr-Mo-C-B-P bulk glassy alloys. *Journal of the Electrochemical Society*. 2002;**149**(8):B366-B369
- [15] Naka M, Hashimoto K, Masumoto T. High corrosion resistance of amorphous Fe-Mo and Fe-W alloys in HCl. *J. Non-Crystalline Solids*. 1978;**30**(1):61-65
- [16] Asami K, Naka M, Hashimoto K, Masumoto T. *Journal of the Electrochemical Society*. 1980;**127**:2130
- [17] Pang SJ, Zhang T, Asami K, Inoue A. Formation of bulk glassy Fe_{75-x-y}Cr_xMo_yC₁₅B₁₀ alloys and their corrosion behavior. *J. Materials Research*. 2002;**17**(3):701-704
- [18] Naka M, Hashimoto K, Masumoto T. Change in corrosion behavior of amorphous Fe-P-C alloys by alloying with various metallic elements. *J. Non-Crystalline Solids*. 1979;**31**(3):355-365
- [19] Wang R. Fall Meeting. Pittsburgh, PA: The Metallurgical Society; 1980

- [20] Shimamura K, Kawashima A, Asami K, Hashimoto K. Corrosion behavior of amorphous nickel-valve metal-alloys in boiling concentrated nitric and hydrochloric acids. *Science Reports of the Research Institutes, Tohoku University*. 1986;**33**(1):196-210
- [21] Mitsunashi A, Asami K, Kawashima A, Hashimoto K. The corrosion behavior of amorphous nickel base alloys in a hot concentrated phosphoric acid. *Corrosion Science*. 1987;**27**(9):957-970
- [22] Lee HJ, Akiyama E, Habazaki H, Kawashima A, Asami K, Hashimoto K. The effect of phosphorus addition on the corrosion behavior of amorphous Ni-30Ta-P alloys in 12 M HCl. *Corrosion Science*. 1995;**37**(2):321-330
- [23] Diegle RB. Crevice Corrosion of Glassy Fe-Ni-Cr-P-B Alloys. *Corrosion*. 1980;**36**(7):362-368
- [24] Pang SJ, Shek CH, Zhang T, Asami K, Inoue A. Corrosion behavior of glassy Ni₅₅Co₅Nb₂₀Ti₁₀Zr₁₀ alloy in 1N HCl solution studied by potentiostatic polarization and XPS. *Corrosion Science*. 2006;**48**(3):625-633
- [25] Habazaki H, Sato T, Kawashima A, Asami K, Hashimoto K. Preparation of corrosion-resistant amorphous Ni-Cr-P-B bulk alloys containing molybdenum and tantalum. *Materials Science and Engineering A*. 2001;**304-306**:696-700
- [26] Pang SJ, Zhang T, Asami K, Inoue A. Bulk glassy Ni(Co)-Nb-Ti-Zr alloys with high corrosion resistance and high strength. *Materials Science and Engineering A*. 2004;**375-377**:368-371
- [27] Hashimoto K, Kasaya M, Asami K, Masumoto T. *Corrosion Engineering*. 1977;**26**:445
- [28] Latanision RM, Turn JC, Comeau CR. In: *Proceedings of the Third International Conference on Mechanical Behavior of Metals*. Vol. 2. 1979. p. 475
- [29] Pang SJ, Zhang T, Asami K, Inoue A. Synthesis of Fe-Cr-Mo-C-B-P bulk metallic glasses with high corrosion resistance. *Acta Mater*. 2002;**50**(3):489-497
- [30] Lin XH, Johnson WL. Formation of Ti-Zr-Cu-Ni bulk metallic glasses. *Journal of Applied Physics*. 1995;**78**(11):6514-6519
- [31] Inoue A, Zhang W, Zhang T, Kurosaka K. High-strength Cu-based bulk glassy alloys in Cu-Zr-Ti and Cu-Hf-Ti ternary systems. *Acta Materialia*. 2001;**49**(14):2645-2652
- [32] Inoue A, Zhang W, Zhang T, Kurosaka K. Thermal and mechanical properties of Cu-based Cu-Zr-Ti bulk glassy alloys. *Materials Transactions*. 2001;**42**(6):1149-1151
- [33] Asami K, Qin CL, Zhang T, Inoue A. Effect of additional elements on the corrosion behavior of a Cu-Zr-Ti bulk metallic glass. *Materials Science and Engineering A*. 2004;**375-377**:235-239
- [34] Liu B, Liu L. The effect of microalloying on thermal stability and corrosion resistance of Cu-based bulk metallic glasses. *Materials Science and Engineering A*. 2006;**415**(1-2):286-290
- [35] Qin CL, Asami K, Zhang T, Zhang W, Inoue A. Corrosion behavior of Cu-Zr-Ti-Nb bulk glassy alloys. *Materials Transactions*. 2003;**44**(4):749-753

- [36] Qin CL, Zhang W, Asami K, Ohtsu N, Inoue A. Glass formation, corrosion behavior and mechanical properties of bulk glassy Cu-Hf-Ti-Nb alloys. *Acta Materialia*. 2005;**53**(14):3903-3911
- [37] Liu L, Liu B. Influence of the micro-addition of Mo on glass forming ability and corrosion resistance of Cu-based bulk metallic glasses. *Electrochimica Acta*. 2006;**51**(18):3724-3730
- [38] Tam MK, Pang SJ, Shek CH. Effects of niobium on thermal stability and corrosion behavior of glassy Cu-Zr-Al-Nb alloys. *Journal of Physics and Chemistry of Solids*. 2006;**67**(4):762-766
- [39] Qin CL, Zhang W, Kimura H, Asami K, Inoue A. New Cu-Zr-Al-Nb bulk glassy alloys with high corrosion resistance. *Materials Transactions*. 2004;**45**(6):1958-1961
- [40] Inoue A, Zhang T, Nishiyama N, Ohba K, Masumoto T. Preparation of 16 mm diameter rod of amorphous Zr₆₅Al_{7.5}Ni₁₀Cu_{17.5} alloy. *Materials Transactions*. 1993;**34**(12):1234-1237
- [41] Peker A, Johnson WL. A highly processable metallic-glass—Zr_{41.2}Ti_{13.8}Cu_{12.5}Ni_{10.0}Be_{22.5}. *Applied Physics Letters*. 1993;**63**(17):2342-2344
- [42] Asami K, Habazaki H, Inoue A, Hashimoto K. Recent development of highly corrosion resistant bulk glassy alloys. *Materials Science Forum*. 2005;**502**:225-230
- [43] Qin FX, Zhang HF, Deng YF, Ding BZ, Hu ZQ. Corrosion resistance of Zr based bulk amorphous alloys containing Pd. *Journal of Alloys and Compounds*. 2004;**375**(1-2):318-323
- [44] Pang SJ, Zhang T, Asami K, Inoue A. Formation, corrosion behavior, and mechanical properties of bulk glassy Zr-Al-Co-Nb alloys. *Journal of Materials Research*. 2003;**18**(7):1652-1658
- [45] Raju VR, Kühn U, Wolff U, Schneider F, Eckert J, Reiche R, Gebert A. Corrosion behaviour of Zr-based bulk glass-forming alloys containing Nb or Ti. *Materials Letters*. 2002;**57**(1):173-177
- [46] Liu L, Qiu CL, Zou H, Chan KC. The effect of the microalloying of Hf on the corrosion behavior of ZrCuNiAl bulk metallic glass. *Journal of Alloys and Compounds*. 2005;**399**(1-2):144-148
- [47] Gebert A, Mummert K, Eckert J, Schultz L, Inoue A. Electrochemical investigations on the bulk glass forming Zr₅₅Cu₃₀Al₁₀Ni₅ alloy. *Materials and Corrosion*. 1997;**48**(5):293-297
- [48] Mudali UK, Baunack S, Eckert J, Schultz L, Gebert A. Pitting corrosion of bulk glass-forming zirconium-based alloys. *Journal of Alloys and Compounds*. 2004;**377**:290-297
- [49] Hiromoto S, Tsai AP, Sumita M, Hanawa T. Effect of chloride ion on the anodic polarization behavior of the Zr₆₅Al_{7.5}Ni₁₀Cu_{17.5} amorphous alloy in phosphate buffered solution. *Corrosion Science*. 2000;**42**(9):1651-1660
- [50] Gebert A, Buchholz K, El-Aziz AM, Eckert J. Hot water corrosion behaviour of Zr-Cu-Al-Ni bulk metallic glass. *Materials Science and Engineering A*. 2001;**316**(1-2):60-65
- [51] Morrison ML, Buchanan RA, Senkov ON, Miracle DB, Liaw PK. Electrochemical behavior of Ca-based bulk metallic glasses. *Metallurgical and Materials Transactions A*. 2006;**37**(4):1239-1245

- [52] Gebert A, Subba Rao RV, Wolff U, Baunack S, Eckert J, Schultz L. Corrosion behaviour of the Mg₆₅Y₁₀Cu₁₅Ag₁₀ bulk metallic glass. *Materials Science and Engineering A*. 2004;**375-377**:280-284
- [53] Morrison ML, Buchanan RA, Peker A, Liaw PK, Horton JA. Electrochemical behavior of a Ti-based bulk metallic glass. *Journal of Non-Crystalline Solids*. 2007;**353**(22-23): 2115-2124
- [54] Inoue A, Masumoto T. Mg-based amorphous alloys. *Materials Science and Engineering A*. 1993;**173**(1-2):1-8
- [55] Schroeder V, Gilbert CJ, Ritchie RO. Comparison of the corrosion behavior of a bulk amorphous metal, Zr_{41.2}Ti_{13.8}Cu_{12.5}Ni₁₀Be₂₂, with its crystallized form. *Scripta Materialia*. 1998;**38**(10):1481-1485
- [56] Peter WH, Buchanan RA, Liu CT, Liaw PK, Morrison ML, Carmichael CA Jr, Wright JL. Localized corrosion behavior of a zirconium-based bulk metallic glass relative to its crystalline state. *Intermetallics*. 2002;**10**(11-12):1157-1162
- [57] Köster U, Zander D, Triwikantoro RA, Jastrow L. Environmental properties of Zr-based metallic glasses and nanocrystalline alloys. *Scripta Materialia*. 2001;**44**(8-9):1649-1654
- [58] Archer MD, Corke CC, Harji BH. The electrochemical properties of metallic glasses. *Electrochimica Acta*. 1987;**32**(1):13-26
- [59] Ji X, Hu B, Li Y, Wang S. Sliding tribocorrosion behavior of bulk metallic glass against bearing steel in 3.5% NaCl solution. *Tribology International*. 2015;**91**:214-220
- [60] Tian P, Khun NW, Tor SB, Liu E, Tian Y. Tribological behavior of Zr-based bulk metallic glass sliding against polymer, ceramic, and metal materials. *Intermetallics*. 2015;**61**:1-8
- [61] Zhong H, Chen J, Dai LY, Yue Y, Wang BA, Zhang XY, Ma MZ, Liu RP. Effect of counterpart material on the tribological properties of Zr-based bulk metallic glass under relatively heavy loads wear. 2015;**346**:22-28
- [62] Wu H, Baker I, Liu Y, Wu X-l. Dry sliding tribological behavior of Zr-based bulk metallic glass. *Transactions of Nonferrous Metals Society of China*. 2012;**22**(3):585-589
- [63] Tao PJ, Yang YZ, Bai XJ, Ru Q, Xie ZW. Effect of load on linear reciprocating sliding friction and wear behavior in Zr-based bulk metallic glass. *Advanced Materials Research*. 2011;**152-153**:1905-1908
- [64] Wang Y, Shi LL, Duan DL, Li S, Xu J. Tribological properties of Zr₆₁Ti₂Cu₂₅Al₁₂ bulk metallic glass under simulated physiological conditions. *Materials Science & Engineering. C, Materials for Biological Applications*. 2014;**37**:292-304
- [65] Hua N, Zheng Z, Fang H, Ye X, Lin C, Li G, Wang W, Chen W, Zhang T. Dry and lubricated tribological behavior of a Ni- and Cu-free Zr-based bulk metallic glass. *Journal of Non-Crystalline Solids*. 2015;**426**:63-71
- [66] Anis M, Rainforth WM, Davies HA. Wear behaviour of rapidly solidified Fe₆₈Cr₁₈Mo₂B₁₂ alloys. *Wear*. 1994;**172**(2):135-145

- [67] Seifert V, Zimmermann M, Trantakis C, Vitzthum HE, Kuhnel K, Raabe A, Bootz F, Schneider JP, Schmidt F, Dietrich J. OpenMRI-guided neurosurgery. *Acta Neurochirurgica*. 1999;**141**:455-464
- [68] Horton JA, Parsell DE. Biomedical potential of a zirconium-based bulk metallic glass. *MRS Proceedings In: Symposium CC- Supercooled Liquids, Glass Transition and Bulk Metallic Glasses*; Vol. 754, CC1.5; 2002. DOI: 10.1557/PROC-754-CC1.5
- [69] Saotome Y, Hatori T, Zhang T, Inoue A. Superplastic micro/nano-formability of La-60, Al-20, Ni-10, Co-5, Cu-5 amorphous alloy in supercooled liquid state. *Materials Science and Engineering A*. 2001;**304-306**:716-720
- [70] Espallargas N, Aune RE, Torres C, Papageorgiou N, Muñoz AI. Bulk metallic glasses (BMG) for biomedical applications—A tribocorrosion investigation of Zr₅₅Cu₃₀Ni₅Al₁₀ in simulated body fluid. *Wear*. 2013;**301**(1-2):271-279
- [71] Zhao GH, Aune RE, Mao H, Espallargas N. Degradation of Zr-based bulk metallic glasses used in load-bearing implants: A tribocorrosion appraisal. *J. Mechanical Behavior of Biomedical Materials*. 2015;**60**:56-67